

Eccentric protons? Sensitivity of flow to system size and shape in p+p, p+Pb and Pb+Pb collisions

Björn Schenke and Raju Venugopalan

Physics Department, Brookhaven National Laboratory, Upton, NY 11973, USA

We determine the transverse system size of the initial non-equilibrium Glasma state and of the hydrodynamically evolving fireball as a function of produced charged particles in p+p, p+Pb and Pb+Pb collisions at the Large Hadron Collider. Our results are consistent with recent measurements of Hanbury-Brown-Twiss (HBT) radii by the ALICE collaboration. Azimuthal anisotropy coefficients v_n generated by combining the early time Glasma dynamics with viscous fluid dynamics in Pb+Pb collisions are in excellent agreement with experimental data for a wide range of centralities. In particular, event-by-event distributions of the v_n agree with the experimental data out to fairly peripheral centrality bins. In striking contrast, our results for p+Pb collisions significantly underestimate the magnitude and do not reproduce the centrality dependence of data for v_2 and v_3 coefficients. We argue that the measured v_n data and HBT radii strongly constrain the shapes of initial parton distributions across system sizes that would be compatible with a flow interpretation in p+Pb collisions. Alternately, additional sources of correlations may be required to describe the systematics of long range rapidity correlations in p+p and p+Pb collisions.

The description of ultra-relativistic heavy-ion (A+A) collisions with event-by-event viscous fluid-dynamic models has been extremely successful [1]. In particular the color-glass-condensate (CGC) [2] based IP-Glasma model [3, 4] in combination with the viscous fluid dynamic simulation MUSIC [5–7] provides a consistent description of particle spectra, the anisotropic flow coefficients v_n and their event-by-event distributions [8].

Recent measurements at the Relativistic Heavy Ion Collider (RHIC) at Brookhaven National Laboratory (BNL) and the Large Hadron Collider (LHC) at CERN have shown striking similarities in the structure of long range pseudo-rapidity correlations between high-multiplicity deuteron-gold (d+Au) [9] and proton-lead (p+Pb) collisions [10–12] and peripheral heavy-ion collisions with similar multiplicity. One may thus conclude that the small collision systems are dominated by the same physics, namely collective flow of the produced matter. Indeed, first fluid dynamic calculations have been able to describe certain features of the experimental data in d+Au and p+Pb collisions [13–16]. In particular, the observed mass splitting of elliptic flow has been at least qualitatively explained within the fluid dynamic framework [17, 18].

The observed long range correlations in pseudo-rapidity are an input in the fluid dynamic framework while the azimuthal structure follows from the system's collective response to the transverse geometry as in A+A collisions. An explanation of the long range correlations in all collision systems is given in the color-glass-condensate based description of multi-particle production in high energy nuclear collisions [19, 20]. In addition, this description produces a collimation in azimuth that is compatible with experimental data on the associated yield in p+p and p+A collisions, without any final state interactions [21–25].

The important question that needs to be answered

is whether the physics responsible for the observed anisotropic flow in A+A collisions is qualitatively different from that in high-multiplicity p+p and p+A (d+A) collisions, or whether collective effects are always dominant. We argue that in order to conclude the latter, a systematic quantitative description from central to peripheral A+A to p/d+A to p+p collisions needs to be given within the same theoretical framework.

In this letter, we first demonstrate that the IP-Glasma+MUSIC model that provided an excellent description of data for central and mid-central A+A collisions at RHIC and LHC continues to provide a good description of the data as we study more and more peripheral heavy-ion events. This holds not only for the mean values of v_n but also their event-by-event distributions. These results are an important validation of the applicability of our model to A+A collisions especially since a recent study concludes that the v_n distributions are not well described by most other initial state models [26]. We further demonstrate that the system sizes predicted in the IP-Glasma+MUSIC model for p+p, p+A, and A+A collisions are compatible with the experimentally measured Hanbury-Brown-Twiss (HBT) radii [27]. It is however not possible to determine from the radii alone whether fluid dynamic expansion is present in p+p or p+A collisions.

We study finally the multiplicity dependence of elliptic and triangular flow in A+A and p+A collisions. This requires a proper description of the multiplicity distribution for both systems [4, 28]. We find that while the description of v_2 and v_3 in peripheral A+A collisions is fairly good, the theoretical results for p+A collisions underpredict the experimental data by factors of up to 4.

Given the excellent results of the model for A+A collisions and the various system sizes, the result for p+Pb collisions has dramatic implications. Two equally exciting explanations for the disagreement are possible. Previ-

ously discussed multi-particle correlations present in initial gluon production have been ignored in this and all other calculations that are based on collective final state effects. One explanation of our p+Pb results is that these initial state contributions could significantly modify the result for v_2 and v_3 if final state effects are not able to overpower them—the latter seems to be the case in A+A collisions [22]. Alternatively, the disagreement with the measured v_2 and v_3 could stem from simplified assumptions about the (spherical) shape of gluon distributions in the proton¹. Deformed parton distributions in the proton would lead to larger initial eccentricities within our model and could generate significantly larger anisotropic flow. This implies that the new measurements at RHIC and LHC could provide unprecedented insight into the detailed shape of a proton at high energy [30, 31]. We shall later comment on open questions that both these explanations will have to address.

We begin our systematic study by demonstrating that, for a fixed shear viscosity to entropy density ratio $\eta/s = 0.18$, anisotropic flow data from heavy-ion collisions at LHC is well described by fluid dynamic simulations using the IP-Glasma initial state described in [28]. The IP-Glasma energy density and flow velocities serve as input to the fluid dynamic simulation MUSIC as described in [8]. Here we choose the initial time $\tau_0 = 0.4 \text{ fm}/c$ for the fluid dynamic simulation.² We select centralities based on the gluon multiplicity distribution at τ_0 , obtained from $\sim 40,000$ IP-Glasma events. This centrality selection method neglects possible corrections due to entropy production during the fluid dynamic evolution and effects from hadronization. It is however close to the experimental procedure and avoids having to simulate the fluid dynamic evolution for tens of thousands of events. After kinetic freeze-out at $T_{\text{kin fo}} = 135 \text{ MeV}$ (chemical freeze-out occurs at $T_{\text{chem fo}} = 150 \text{ MeV}$) and resonance decays, we determine v_n for $n \in \{2, 3, 4, 5\}$ of charged hadrons in every event by first determining the event-plane angle $\psi_n = (1/n) \arctan(\langle \sin(n\phi) \rangle / \langle \cos(n\phi) \rangle)$, and then computing $v_n = \langle \cos(n(\phi - \psi_n)) \rangle$, where $\langle \cdot \rangle$ are averages over the charged hadron distribution functions.

In Fig. 1 we present results for the mean $\langle v_n \rangle$ as a function of centrality compared to experimental results from the ATLAS collaboration [32]. Here we study significantly more peripheral events than in previous studies [8]. The agreement is excellent from the most central to

50% central events. For more peripheral events our results are up to 10% larger than the experimental data, with differences being largest for v_2 . Between 0% and 20%, the calculated v_3 slightly underestimates the experimental result.

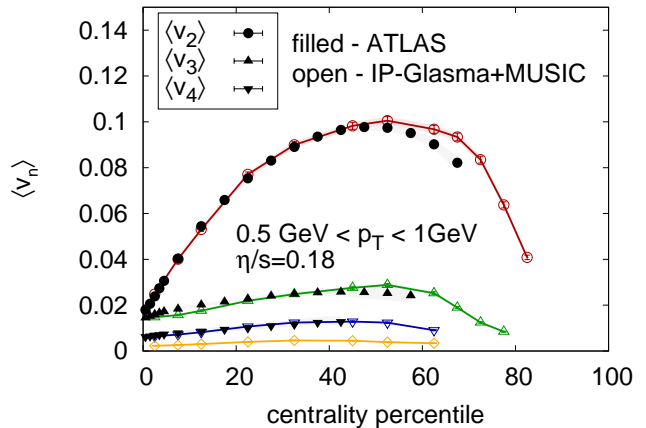


FIG. 1. (Color online) The event averaged p_T -integrated $\langle v_n \rangle$ as a function of centrality compared to experimental data from the ATLAS collaboration [32].

We next present the computed event-by-event distributions of v_2 , v_3 , and v_4 and the corresponding initial state eccentricities defined as $\varepsilon_n = \sqrt{\langle r^n \cos(n\phi) \rangle^2 + \langle r^n \sin(n\phi) \rangle^2} / \langle r^n \rangle$, where $\langle \cdot \rangle$ is the average weighted by the deposited energy density. We compare to data in the respective maximally peripheral bin measured by the ATLAS collaboration [32]. All distributions are scaled by their mean value. More central bins have been studied previously in [8].

The ε_3 distribution already provides a good description of the measured v_3 distribution, while ε_2 and ε_4 distributions are significantly narrower. However, non-linear effects in the fluid dynamic evolution modify the shape of the distributions such that the calculated v_n distributions agree with the experimental result. This result strongly supports the importance of fluid dynamics in heavy-ion collisions. We have checked that the scaled distributions are only weakly dependent of the value of η/s , as was previously found in [33].

Having established that even fairly peripheral events are well described by the IP-Glasma+MUSIC model, we now move on to applying the model to p+Pb and p+p collisions. We shall first determine whether the predicted system size (with and without fluid dynamical expansion) is consistent with HBT measurements for all systems.

To be able to compare the initial size as well as the maximal size of the system during the evolution to the measured HBT radii, we define r_{max} as the (angle-averaged) radius where the system reaches the minimal threshold energy density ε_{min} . This defines a size equivalent to the size of the system at freeze-out at a given

¹ Gluon distributions in the proton are extracted from fits of model parameters to combined H1 and ZEUS data on inclusive structure functions. These give excellent χ -squared fits to diffractive and exclusive HERA data [29]. However, these data may not fully capture the shapes of gluon distributions.

² The effects of varying τ_0 have been studied previously. They are small even if τ_0 is decreased by a factor of two [8]. Increasing τ_0 beyond the quoted value will, in this framework, impact the amount of flow generated.

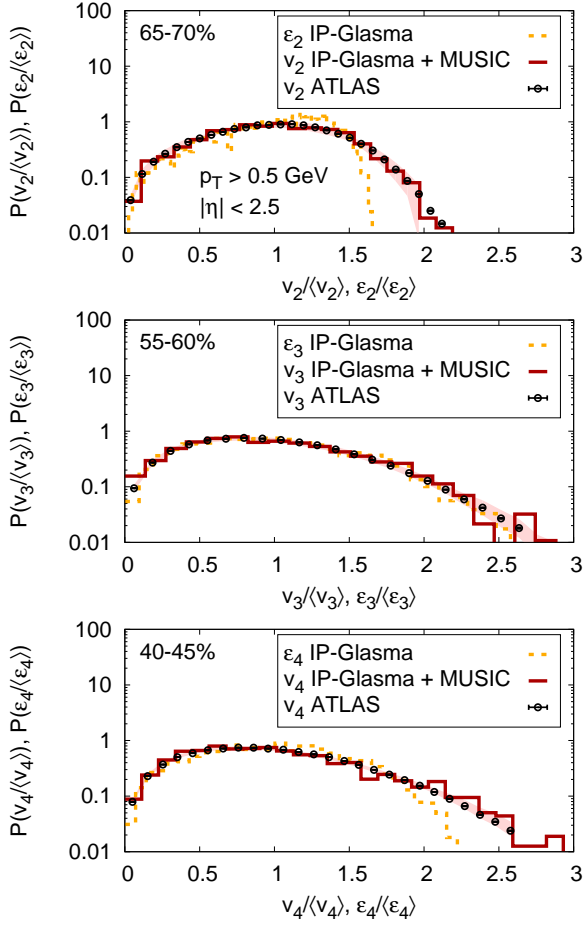


FIG. 2. (Color online) Data points correspond to the event-by-event distribution of v_2 , v_3 , and v_4 in the respective maximal peripheral bin measured by the ATLAS collaboration [32]. These are compared to the distributions of initial eccentricities in the IP-Glasma model and the distributions of v_n from fluid dynamic evolution with IP-Glasma initial conditions.

energy density. This radius by definition depends on the choice of ε_{\min} . This choice however only affects the overall normalization of r_{\max} ; it does not affect the dependence of r_{\max} on the number of charged particles N_{ch} [34]. There is also some uncertainty in the radii coming from the choice of the infrared scale m that regulates the long distance tail of the gluon distribution (see [3, 4, 28]). It can be mostly compensated for by adjusting a normalization constant K .

In Fig. 3 we show the result for r_{\max} in p+p, p+Pb, and Pb+Pb collisions and compare to R_{inv} from the Edgeworth fit to the two-pion correlation function measured by the ALICE collaboration [27]. We adjust K to match to the p+p results. We determine centrality classes in the model and assign the N_{ch} value quoted by ALICE [27] for each centrality class.

Because the emission of pions occurs throughout the

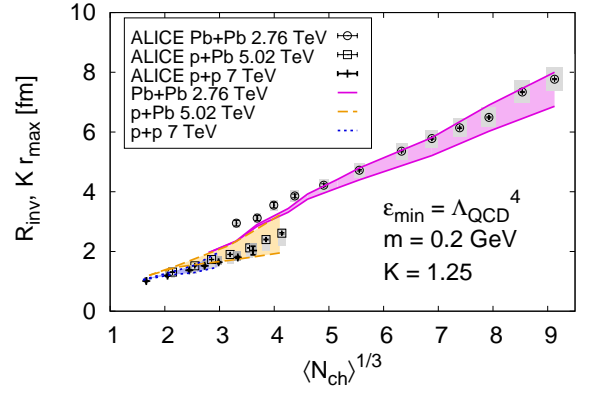


FIG. 3. (Color online) R_{inv} measured by the ALICE collaboration [27] compared to Kr_{\max} determined using the IP-Glasma model and fluid dynamic expansion. The lower end of the band indicates the size of the initial state, the upper end the maximal value of r_{\max} during the hydrodynamic evolution.

evolution, R_{inv} lies somewhere between the initial radius and the maximal radius reached during evolution. We indicate the range of radii between these two extrema by a band in Fig. 3. We find that our estimate of the system size is compatible with the experimental HBT measurement for all systems simultaneously. The Pb+Pb result clearly favors the presence of hydrodynamic expansion.

For events with the same multiplicity (for example at $\langle N_{\text{ch}} \rangle^{1/3} \approx 4$), p+Pb collisions in the hydrodynamic framework show a much more significant expansion compared to Pb+Pb collisions. For these high multiplicities, hydrodynamic expansion in p+Pb collisions appears to be necessary to explain the experimental data. However, using $m = 0.1$ GeV instead of $m = 0.2$ GeV leads to larger initial radii that are also compatible with the experimental data.

We have established that the details of the bulk properties in Pb+Pb collisions as well as the systematics of the system size from p+p to Pb+Pb collisions are well reproduced in the IP-Glasma (+fluid dynamics) model. We turn now to address anisotropic flow in p+Pb collisions. Using the same method as in Pb+Pb collisions, we determine v_2 and v_3 as a function of $N_{\text{trk}}^{\text{offline}}$, measured by the CMS collaboration.³

Fig. 4 shows the calculated v_2 in peripheral Pb+Pb collisions and central p+Pb collisions with the same $N_{\text{trk}}^{\text{offline}}$ in comparison to experimental data by the CMS collaboration [35]. While the Pb+Pb result reproduces the

³ To obtain $N_{\text{trk}}^{\text{offline}}$ we determine the centrality class in the IP-Glasma simulations and match to the $N_{\text{trk}}^{\text{offline}}$ quoted for that centrality class by the CMS collaboration in [35]. $N_{\text{trk}}^{\text{offline}} \approx 132$ corresponds to 65-70% central Pb+Pb events, the most peripheral bin shown for the ATLAS data in Fig. 1.

experimental data within 10-15%, the computed v_2 in p+Pb collisions underestimates the data by a factor of approximately 3.5. We have checked that even in the ideal case ($\eta/s = 0$) the data is still underestimated by approximately a factor of 2. We also varied the freeze-out temperature and switching time τ_0 , but no choice of parameters could achieve much better agreement with the experimental data. For v_3 , shown in Fig. 5, we find a similar result: Pb+Pb data are well described, while p+Pb data are underestimated for $N_{\text{trk}}^{\text{offline}} > 60$. Ideal fluid dynamics (not shown) increases the v_3 significantly by nearly a factor of 4. Its $N_{\text{trk}}^{\text{offline}}$ dependence is rather flat, slightly decreasing with increasing $N_{\text{trk}}^{\text{offline}}$, opposite to the trend seen in the experimental data.

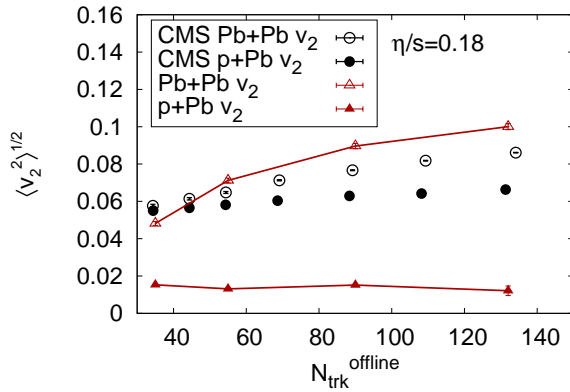


FIG. 4. (Color online) Multiplicity dependence of the root-mean-square elliptic flow coefficient v_2 in Pb+Pb (open symbols) and p+Pb collisions (filled symbols) from the IP-Glasma+MUSIC model (connected triangles) compared to experimental data by the CMS collaboration [35].

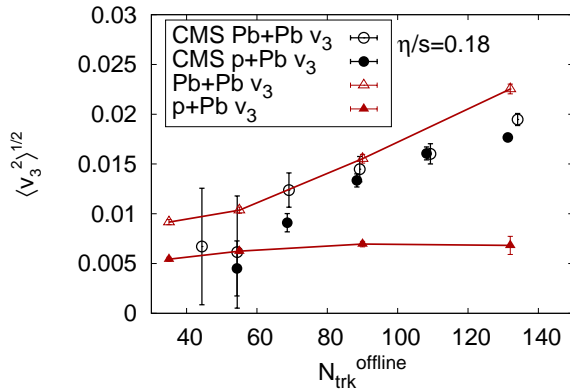


FIG. 5. (Color online) Multiplicity dependence of the root-mean-square triangular flow coefficient v_3 in Pb+Pb (open symbols) and p+Pb collisions (filled symbols) from the IP-Glasma+MUSIC model (connected triangles) compared to experimental data by the CMS collaboration [35].

The primary reason for the small v_n in p+Pb collisions is that the initial shape of the system closely follows the shape of the proton (see [34]), which is spherical in our model. The subnucleonic fluctuations included generate non-zero values of the v_n , but they do not fully account for the larger experimentally observed values. As noted above, modifications of the (fluctuating) proton shape are necessary to account for the larger observed v_2 and v_3 in p+Pb collisions. If the hydrodynamic paradigm is valid, the results of the high-multiplicity p+Pb and p+p collisions could then in principle be used to extract detailed information on the spatial gluon distribution in the proton.

There are hydrodynamical models that describe aspects of the p+Pb data. These models should also describe key features of Pb+Pb collisions where hydrodynamics is more robust. A model where the spatial geometry of p+Pb collisions is different from ours is that of [13–17], where the interaction region is determined from the geometric positions of participant nucleons. However, as noted, this model falls into the class of models that are claimed [26] not to be able to reproduce the data on event-by-event v_n distributions in A+A collisions. Whether this particular model can do so needs to be examined. We also note that the v_2 centrality dependence in the model differs from the CMS data for p+Pb collisions [16].

Another model which claims large v_2 and v_3 in p+Pb collisions determines the system size from the position of “cut pomerons” and strings [18, 36]. The multiplicity dependence of the v_n in this model has not yet been shown. The v_n distributions in A+A collisions should also provide a stringent test of this model.

In addition to the important quantitative tests imposed on different hydrodynamical models by the experimental data, there are conceptual issues that arise due to the possible breakdown of the hydrodynamic paradigm when extended to very small systems. As shown in recent quantitative studies, viscous corrections can be very significant in p+Pb collisions but play a much smaller role in Pb+Pb collisions [34, 37]. In particular, an analysis of Knudsen numbers reached during the evolution in A+A and p+A collisions finds that viscous hydrodynamics breaks down for $\eta/s \geq 0.08$ in p+A collisions [37].

An alternative to the hydrodynamic picture and its sensitivity to the proton shape is provided within the Glasma framework itself by initial state correlations of gluons that show a distinct elliptic modulation in relative azimuthal angle [21–25]. If these are not overwhelmed in p+Pb collisions by final state effects, as they are in A+A collisions, they can contribute significantly to the observed v_2 , and possibly v_3 . The initial state correlations are those of gluons and do not address features of the data such as the mass ordering in particle spectra. While natural in hydrodynamical models, mass ordering may also emerge due to universal hadronization effects,

as demonstrated in a string model [38].

In summary, we have shown that the IP-Glasma model in combination with fluid dynamics describes very well the Fourier coefficients of the azimuthal particle distributions in Pb+Pb collisions out to fairly peripheral collisions. Both the experimental mean values and event-by-event distributions are well reproduced. The systematics of HBT radii in p+p, p+A, and A+A collisions are also well described. The discrepancy of our results with the experimental v_2 and v_3 data in p+Pb collisions therefore poses a challenge to applying the hydrodynamic paradigm to such small systems. A possible solution within the hydrodynamic framework could result from the inclusion of additional shape fluctuations of gluon distributions in both p+p and p+Pb collisions. Initial state effects that are also present in the Glasma framework may provide an alternative explanation of the noted discrepancy between experimental data and theory. These conclusions point to the importance of a deeper understanding of spatial shapes, sizes and correlations of gluon distributions in high energy QCD.

ACKNOWLEDGMENTS

This research used resources of the National Energy Research Scientific Computing Center, which is supported by the Office of Science of the U.S. Department of Energy under Contract No. DE-AC02-05CH11231. BPS and RV are supported under DOE Contract No. DE-AC02-98CH10886.

-
- [1] C. Gale, S. Jeon, and B. Schenke, Int. J. of Mod. Phys. A, Vol. 28, **1340011** (2013), arXiv:1301.5893 [nucl-th].
 - [2] F. Gelis, E. Iancu, J. Jalilian-Marian, and R. Venugopalan, Ann.Rev.Nucl.Part.Sci. **60**, 463 (2010).
 - [3] B. Schenke, P. Tribedy, and R. Venugopalan, Phys. Rev. Lett. **108**, 252301 (2012).
 - [4] B. Schenke, P. Tribedy, and R. Venugopalan, Phys. Rev. **C86**, 034908 (2012).
 - [5] B. Schenke, S. Jeon, and C. Gale, Phys. Rev. **C82**, 014903 (2010).
 - [6] B. Schenke, S. Jeon, and C. Gale, Phys. Rev. Lett. **106**, 042301 (2011).
 - [7] B. Schenke, S. Jeon, and C. Gale, Phys. Rev. **C85**, 024901 (2011).
 - [8] C. Gale, S. Jeon, B. Schenke, P. Tribedy, and R. Venugopalan, Phys.Rev.Lett. **110**, 012302 (2013).
 - [9] A. Adare et al. (PHENIX Collaboration), (2013), arXiv:1303.1794 [nucl-ex].
 - [10] S. Chatrchyan et al. (CMS Collaboration), Phys.Lett. **B718**, 795 (2013), supplemental materials: <https://twiki.cern.ch/twiki/bin/view/CMSPublic/PhysicsResultsHIN12015>, arXiv:1210.5482 [nucl-ex].
 - [11] B. Abelev et al. (ALICE Collaboration), Phys.Lett. **B719**, 29 (2013), arXiv:1212.2001 [nucl-ex].
 - [12] G. Aad et al. (ATLAS Collaboration), (2012), arXiv:1212.5198 [hep-ex].
 - [13] P. Bozek, Phys.Rev. **C85**, 014911 (2012).
 - [14] P. Bozek and W. Broniowski, Phys.Lett. **B718**, 1557 (2013), arXiv:1211.0845 [nucl-th].
 - [15] P. Bozek and W. Broniowski, (2013), arXiv:1301.3314 [nucl-th].
 - [16] P. Bozek and W. Broniowski, Phys.Rev. **C88**, 014903 (2013), arXiv:1304.3044 [nucl-th].
 - [17] P. Bozek, W. Broniowski, and G. Torrieri, Phys.Rev.Lett. **111**, 172303 (2013), arXiv:1307.5060 [nucl-th].
 - [18] K. Werner, M. Bleicher, B. Guiot, I. Karpenko, and T. Pierog, (2013), arXiv:1307.4379.
 - [19] F. Gelis, T. Lappi, and R. Venugopalan, Phys. Rev. **D79**, 094017 (2008).
 - [20] K. Dusling, F. Gelis, T. Lappi, and R. Venugopalan, Nucl. Phys. **A836**, 159 (2010), arXiv:0911.2720 [hep-ph].
 - [21] A. Dumitru, K. Dusling, F. Gelis, J. Jalilian-Marian, T. Lappi, and R. Venugopalan, Phys. Lett. **B697**, 21 (2011), arXiv:1009.5295 [hep-ph].
 - [22] K. Dusling and R. Venugopalan, Phys.Rev.Lett. **108**, 262001 (2012), arXiv:1201.2658 [hep-ph].
 - [23] K. Dusling and R. Venugopalan, (2012), arXiv:1210.3890 [hep-ph].
 - [24] K. Dusling and R. Venugopalan, (2012), arXiv:1211.3701 [hep-ph].
 - [25] K. Dusling and R. Venugopalan, Phys.Rev. **D87**, 094034 (2013), arXiv:1302.7018 [hep-ph].
 - [26] T. Renk and H. Niemi, (2014), arXiv:1401.2069 [nucl-th].
 - [27] B. B. Abelev et al. (ALICE Collaboration), (2014), arXiv:1404.1194 [nucl-ex].
 - [28] B. Schenke, P. Tribedy, and R. Venugopalan, (2013), arXiv:1311.3636 [hep-ph].
 - [29] A. H. Rezaeian, M. Siddikov, M. Van de Klundert, and R. Venugopalan, Phys.Rev. **D87**, 034002 (2013).
 - [30] G. A. Miller, Nucl.Phys.News **18**, 12 (2008), arXiv:0802.3731 [nucl-th].
 - [31] J. D. Bjorken, S. J. Brodsky, and A. Scharff Goldhaber, Phys.Lett. **B726**, 344 (2013), arXiv:1308.1435 [hep-ph].
 - [32] G. Aad et al. (ATLAS Collaboration), JHEP **1311**, 183 (2013), arXiv:1305.2942 [hep-ex].
 - [33] H. Niemi, G. Denicol, H. Holopainen, and P. Huovinen, Phys.Rev. **C87**, 054901 (2013), arXiv:1212.1008 [nucl-th].
 - [34] A. Bzdak, B. Schenke, P. Tribedy, and R. Venugopalan, Phys.Rev. **C87**, 064906 (2013), arXiv:1304.3403 [nucl-th].
 - [35] S. Chatrchyan et al. (CMS Collaboration), Phys.Lett. **B724**, 213 (2013), arXiv:1305.0609 [nucl-ex].
 - [36] K. Werner, B. Guiot, I. Karpenko, and T. Pierog, (2013), arXiv:1312.1233 [nucl-th].
 - [37] H. Niemi and G. Denicol, (2014), arXiv:1404.7327 [nucl-th].
 - [38] A. Ortiz Velasquez, P. Christiansen, E. Cuautle Flores, I. Maldonado Cervantes, and G. Paic, Phys.Rev.Lett. **111**, 042001 (2013), arXiv:1303.6326 [hep-ph].